Raman study of Si nanoparticles formation in the annealed SiO_x and SiO_x:Er,F films on sapphire substrate

A.S. NIKOLENKO, M.V. SOPINSKYY*, V.V. STRELCHUK, L.I. VELIGURA, V.V. GOMONOVYCH
V. Lashkaryov Institute of Semiconductor Physics, NASU, Kyiv, Ukraine

In this work the silicon nanoparticle formation caused by structural-phase transformations in the SiO_x and SiO_x:Er,F films evaporated onto sapphire substrate is studied. These transformations are induced by moderate temperatures annealing (650–1000°C). It was established that the crystallization of a-Si nanoparticles is much more intensive in the annealed SiO_x:Er,F films as compared to the annealed SiO_x films, and the origination of crystalline silicon phase takes place near the interface SiO_x:Er,F film/Al_2O_3 substrate. The obtained results are explaining based on analysis of available literature data on behaviour of Er and F in silicon and Si−O systems.

(Received October 17, 2011; accepted February 20, 2012)

Keywords: Nanostructures, Erbium, Silicon, SiO_2, Fluorine

1. Introduction

Both nc-Si/SiO_2 and erbium doped nc-Si/SiO_2 nanosystems are considered as possible candidates for the manufacturing of light emitting sources compatible with silicon technology [1]. The Er^{3+} ions produce radiation from the 4f shell in a transition from the $^4I_{13/2}$ first excited state to the $^4I_{15/2}$ ground state at 1.54 μm wavelength, one of the standard wavelengths in telecommunications. As shown in [2,3], in structures with erbium ions and Si nanocrystals in SiO_2 matrix both optical and electrical pumping occur by energy transfer from the Si-nanocrystals to the rare-earth ions.

It is attractive to use a simple and cheap technology of formation of nc-Si/SiO_2 and Er-doped nc-Si/SiO_2 light-emitting structures by thermal evaporation of silicon monoxide and thermal coevaporation of SiO and ErF_3, correspondingly. Er-doping by SiO/ErF_3 coevaporation is interesting for two reasons. First, the valency of rare-earth ions is usually +3, which makes charge compensation necessary. Specifically, the fluorine anions can be used for this purpose. Second, as a rule, to form nc-Si/SiO_2 system by means of phase separation in thermally deposited SiO_x films, the temperatures higher than 1000 °C are required. Fluorine, like other halogens, has a tendency to enhance recrystallization processes. Therefore, one could hope that introduction of F will intensify the transformation of amorphous silicon nanoinclusions formed during the initial stage of SiO_x thermal decomposition into Si nanocrystallines, and reduce the low-temperature threshold of this process. Lowering the process temperature is the essential advantage of every technology. In case of SiO_x:Er,F films this is fundamentally important because the segregation of erbium ions into metallic clusters takes place at $T_{ann} > 900$ ˚C. Consequently, the final stage of forming the erbium-doped light-emitting system should not exceed 1000 °C.

It is known that the properties of thin-film systems depend rather strongly on the substrate type. For example, different sizes of Si nanocrystallites and volume fractions of crystalline phase were obtained in the nano-silicon thin films deposited on a-Si, Si_3N_4 and SiO_2 film substrates in the same PECVD run [4]. Also, different spectral distribution and intensity of photoluminescence have been observed after high-temperature annealing of silicon-rich oxide films synthesized under exactly the same conditions on silicon and sapphire substrates [5, 6]. Moreover, very recently authors [7] revealed the differences in structure and luminescent properties of nc-Si–SiO_x light emitting nanosystems formed in the same technological cycle on Si substrates with (100) and (111) crystallographic orientations. The majority of investigations of the silicon nanoinclusion formation in SiO_x films are performed using the samples on monocrystalline silicon substrates. Behaviour of Si-nanosystems on sapphire substrates is less studied as compared to silicon substrates. However, this issue is of great practical importance because sapphire substrates have distinct advantages over crystalline Si (c-Si) ones – they provide better electrical insulation and radiation resistance properties. Such properties of sapphire substrates ensure improved operational characteristics of the nanosytems [8, 9].

The stated shows the importance and actuality of the study of silicon nanoparticle formation process by using thermal annealing of SiO_x and SiO_x:Er,F films deposited on sapphire substrate. Raman spectroscopy is one of the most power tools for such type of investigations [10].

2. Experimental

The SiO_x:ErF_3 initial samples were fabricated by thermal coevaporation from separate sources of 99.9% pure silicon monoxide SiO (Cerac Inc.) and pure ErF_3 onto polycrystalline polished sapphire substrates heated to

150°C in 10^{-3} Pa vacuum. Non-doped SiO_x films were also evaporated for comparison. ErF_3 concentration (C) was 1 mol.%. After deposition the samples were annealed during one hour in air at temperatures of 650–1000°C and in 10^{-3} Pa vacuum at 650°C. Micro-Raman spectra (RS) in the spectral range 100–1800 cm^{-1} were registered at room temperature and 514 nm excitation wavelength using Horiba Jobin-Yvon T-64000 Raman spectrometer. Olympus 50X/0.75 microscope objective was used at excitation power of 1 mW. The spectral resolution was less than 0.02 cm^{-1}.

3. Results

RS of doped and undoped films are shown on Fig. 1a,b. The RS of the initial samples as well as the samples annealed at 650ºC (Fig. 1a,b) display only the bands related to A_{1g} and E_g vibrations of Al_2O_3 which are attributed to scattering in sapphire substrate. Raman spectrum from amorphous silicon in this case was not registered. This may testify to strong bond-angle and bond-length disorder of Si–Si bonds within two-three coordination spheres (clusters of a-Si are absent).

This situation changes radically after annealing at 750ºC. The phonon TA, LA, LO, TO modes caused by Raman scattering in a-Si (a-SiO_x) are registered in RS (Fig. 1a,b). Appearance of phonon spectrum of amorphous silicon points out the thermally stimulated morphological changes in SiO_x and SiO_x:ErF_3 films due to the formation of distinctly expressed a-Si cluster structure (without presence of nanocrystalline nc-Si inclusions). The peak at about 480 cm^{-1} due to the Si–Si TO vibrations is sensitive to the short-range disorder of a-Si. An increase in the width at half-maximum of TO band (Γ_{TO}) and a shift of TO position (ω_{TO}) towards lower frequencies indicate the increase in the short-range disorder [11, 12]. The peak at about 150 cm^{-1}, the Si–Si transverse-acoustical-like (TA) vibrations, is related to the intermediate-range disorder of the films. A decrease in the ratio of the intensity of the TA band to that of the TO band, I_{TA}/I_{TO}, indicates an increase in the intermediate-range order [13]. Considerable intensity of TA band at 150 cm^{-1} as compared to the intensity of TO band at 480 cm^{-1} provides additional evidence that the small-size regions with structural features of amorphous Si are formed. Since the a-Si nanocluster size is comparable to (or less than) the TO phonon wavelength value, the intensity of this band decreases. The presence of coordination defects is necessary for the existence of the longitudinal-acoustic-like (LA) mode at 300 cm^{-1} and the longitudinal-optical-like (LO) mode at 410 cm^{-1}; the more defects the larger values of I_{LA}/I_{TO} and I_{LO}/I_{TO} ratio [14]. The increase in the I_{TO}/I_{TA} value from 0.96 to 1.11, the shift in ω_{TO} towards the higher frequency by about 4 cm^{-1}, and the narrowing of Γ_{TO} by about 15 cm^{-1} in SiO_x:Er,F as compared to SiO_x indicate that the amorphous network in SiO_x:ErF_3 becomes more orderly on both short and intermediate scales.

Increasing the T_{ann} to 1000 ^{0}C for SiO_x film (Fig. 1a) causes the significant decrease of the intensity of the inelastic scattering. This could be caused by increase in the structural disorder of Si–Si bonds and/or additional oxidation of starting SiO_x film (increasing relative concentration of oxygen x). Increase of the substrate signal testifies to decrease of the absorption of exiting laser beam (which can be caused by atmospheric oxidation of a-Si nanoinclusions). An essentially different situation takes place for doped SiO_x:E,F films (Fig. 1b). Significant decrease of scattered intensity from a-Si, and appearance of intense, relatively sharp (half-with 10.3 cm^{-1}) band at 522.4 cm^{-1} is observed in Raman spectra of these films. This shows the presence of nc-Si phase along with a-Si phase in the samples. The ratio of the integrated intensity of the optical phonon bands for a-Si (I_a) and nc-Si (I_{nc}) can be used to estimate the content of nc-Si k_{nc} ((nc-Si)/(a-Si) ratio) [15]. In our case $k_{nc} = I_{nc}/(I_{nc}+I_a) = 0.37$.

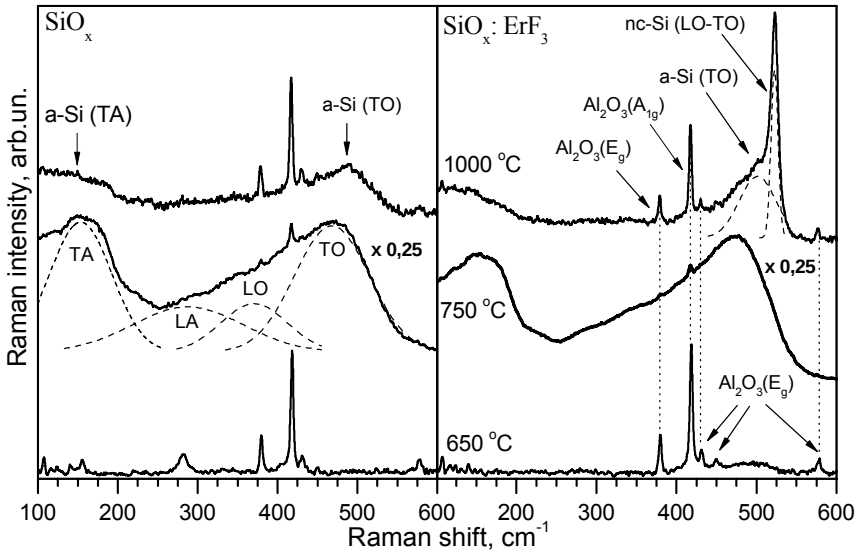

Fig. 1. Micro-Raman spectra of the SiO_x and SiO_x:ErF_3 films annealed in air for 1 hour at 650, 750 and 1000^{0}C.

In Raman spectra, the optical phonon peak of nc-Si is red-shifted and broadened as compared to monocrystalline Si. Based on Richter's model [16], the Raman intensity of the optical phonon of spherical nc-Si particles (< 20 nm) can be expressed as [17]:

$$I(\omega) = \int_0^1 \frac{\exp(-q^2 L^2 / 4a^2)}{\left[\omega - \omega(q)\right]^2 + (\Gamma_0 / 2)^2} d^3 q \qquad (1)$$

where $\omega(q)$ is the dispersion relation of the TO phonon; for Si, $\omega(q)$ equals $[A + B\ cos\ (\pi q/2)]^{1/2}$, with $A = 1.714\times10^5$ cm^{-2} and $B = 1.000\times10^5$ cm^{-2}. q is the wave vector of the phonon in $2\pi/a_0$, and a_0 (0.543086 nm for Si) is the lattice constant. Γ_0 is the natural line width (3.6 cm^{-1} for Si), and L is the average diameter of the spherical nc-Si particles. From the approximation of the nanocrystalline component of experimental spectrum by the Eq. (1), it was found that the average size of Si nanocrystals formed at 1000 °C annealing of SiO_x:Er,F films is $L = 7$ nm. For crystallites of such size the red shift of the phonon band caused by size-induced confinement should be of the 4 cm^{-1} order [17]. However, in our case the 1.4 cm^{-1} blue shift relatively to Si bulk phonon frequency (521 cm^{-1}) is observed. Thus, the total up-shift amounts to 5.4 cm^{-1}. Mechanical strain or stress may affect the frequencies of the Raman modes. The total 5.4 cm^{-1} up-shift indicates the existence of the compressive stress in the Si-nanocrystals acting in the opposite direction of the phonon confinement effect [18]. In case of biaxial stress in the x–y plane, with stress components σ_{xx} and σ_{yy}, assuming that the relation between Raman shift and stress is linear, this becomes [19]:

$$\Delta\omega(cm^{-1}) = -4\times10^{-9}\left(\frac{\sigma_{xx} + \sigma_{yy}}{2}\right)(Pa) \qquad (2)$$

This estimate in our case gives σ ≈ -1.3 GPa.

4. Discussion

Since SiO_x:Er,F films have not been studied before, we will analyze the obtained results based on available literature data which deal with doping of Si−O systems and silicon with Er, F, and trifluorides of rare earth metals. Data on the formation of Si−O thin films on silicon and sapphire will also be used.

Taking into consideration the results of comprehensive studies of the SiO_x:Tb,F films obtained by simultaneous co-evaporation of SiO and TbF_3 [20, 21] and similarity of thermodynamic properties of ErF_3 and TbF_3 [22] one should bare in mind that in our SiO_x:Er,F films Er and F can be incorporated into the as-deposited film not only in the form of ErF_3 quasimolecular complexes but also in other configurations. One can expect that the most pronounced differences in structural and physical-chemical properties of SiO_x and SiO_x:Er,F would be due to presence of atomic and bounded fluorine in the SiO_x:Er,F films. This is due to two circumstances: first, fluorine has high mobility in SiO_2 and silicon [23–25]; and second, it saturates the dangling bonds of Si and O [26, 27]. The last circumstance, in particular, explains the presence of smaller number of dangling bonds in as-prepared SiO_x:Er,F films as compared to as-prepared SiO_x films (which is confirmed by EPR measurements on our films [28]). Both of these circumstances cause greater intensity of the near-band photoluminescence of c-Si substrates covered by SiO_x:Er,F films as compared to near-band photoluminescence of c-Si substrates covered by SiO_x films [29].

As our experimental results show, codeposition of ErF_3 enhances formation of Si nanocrystallites, and retards oxidation of SiO_x. Both the difference in degree of oxidation and the degree of the Si nanoinclusion formation grow with increase in annealing temperature. These facts correlate with temperature dependence of dissociation of ErF_3 quasimolecular complexes(centers) – the dissociation increases with increase in temperature, resulting in the increase of amount of active non-bonded fluorine in SiO_x:Er,F films similar to ZnS: Er,F films [30]. It is known that random crystallization rate in a-Si can be enhanced enormously by the presence of fluorine [31]. In [32–34] it was established that introduction of even small quantities of fluorine while producing amorphous silicon films by plasma enhanced chemical vapour deposition induces a formation of crystalline phase, and leads to appearance of 3–9 nm and large Si-nanocrystallines in such a films without additional annealing.

We presume that in our case the mechanism of fluorine influence on the crystallization in annealed SiO_x:Er,F films is similar to the mechanism of hydrogen-induced crystallization of amorphous Si thin films [35] – that is, the main factor that stimulates crystallization is fluorine insertion into strained Si–Si bonds and between two Si atoms that are not bonded to each other. In the fist the Si–Si bond is relaxed and the Si–Si bond length becomes closer to the equilibrium bond length in crystalline Si after the F atom leaves the bridging configuration. In the second case, after the F diffuses away from this bond-center position, a Si–Si bond is formed between these previously nonbonded Si atoms. Both events enhance disorder-to-order transition.

Significant intrinsic compressive stress (up to 1 GPa) was measured in Si:H films on c-Si substrate grown just before the transition to microcrystalline material (that is, in films containing both crystalline and amorphous phases) [36]. One reason for high stress value is that it is generated by unbonded hydrogen. The films are in a state in which SiH_x complexes are formed by H insertion into strained Si-Si bonds increasing intrinsic stress [37,38]. The presence of F atoms enhances this effect and μc-Si:F:H nucleation is initiated [39]. In the intermediate (containing both amorphous and crystalline phases) RF PECVD grown μc-Si:F:H films on the Si substrates the value of intrinsic structure-related compressive stress was found to reach up to 4 GPa [39].

The total stress in a thin film deposited on a thick, rigid substrate is the sum of contributions from any

external stress, the intrinsic stress, and the thermal stress [40]:

$$\sigma_t = \sigma_{ext} + \sigma_{int} + \sigma_{th} \quad (3)$$

Due to difference in the thermal expansion coefficient of the substrate and the film ($\alpha_s - \alpha_f$), the thermal stress σ_{th} is built up during cooling of the sample from the annealing temperature T_{ann} to the temperatures at which the stress is measured T_{meas}. This is expressed by [41]

$$\sigma_{th} = E_f/(1 - \nu_f) \cdot (\alpha_f - \alpha_s) \cdot (T_{ann} - T_{meas}) \quad (4)$$

E_f is the elastic (Young's) modulus of the thin film and ν_f is the Poisson ratio.

The compressive thermal stress is the main contributor to lattice strain of epitaxial c-Si films on sapphire (classic SOS systems) because the external stress caused by the c-Si–c-Al_2O_3 lattice mismatch (reaching more than 10%) is unimportant - it relaxes through generation of many structural defects near the interface [42]. However, low external stress is not necessarily the case for the Si nanocrystallites on sapphire substrate. Besides, intrinsic stress in nc-Si can exist.

To estimate the thermally induced stress in 1000^0C annealed SiO_x:Er,F films on sapphire we calculated σ_{th} for the films of *c*-Si, *a*-Si, and *a*-SiO_2 annealed at 1000^0C and measured at $T_{meas} = T_{room}$. The following values of the parameters were used: $\alpha_s = 5.8*10^{-6}$ K^{-1}; $\alpha_f = 2.6*10^{-6}$, $4*10^{-6}$, $4*10^{-7}K^{-1}$ for c-Si, *a*-Si, and *a*-SiO_2, correspondingly; E_f = 112, 80, 73 GPa for c-Si, *a*-Si, and *a*-SiO_2, correspondingly; ν_f = 0.28, 0.20, 0.165 for c-Si, *a*-Si, and *a*-SiO_2, correspondingly. From the relation (4) such σ_{th} values were obtained: –0.50, –0.18, –0.47 GPa for the films of c-Si, *a*-Si, and SiO_2, correspondingly. As we can see, these values correspond to compressive stress. However, their magnitudes are lower than those obtained for the Si nanocrystals in annealed SiO_x:Er,F film.

In [43] the magnitudes of the compressive stress for the Si nanocrystals formed in α–Al_2O_3 by annealing of Si-implanted α–Al_2O_3 at 900 – 1100°C were approximately 1.66–2.57 GPa. It was found that the amount of stress is greater in the smaller nanocrystals formed at lower temperatures; it reaches almost a constant value when the nanocrystal formation process is completed. Similar results for Si-implanted α–Al_2O_3 were also obtained in [44]. Since for the thermal stress the inverse dependence should be valid, such behaviour of the stress for nc-Si in α–Al_2O_3 is caused by the presence of significant internal and/or external stress components.

For our SiO_x:Er,F film annealed at 1000°C the sum $\sigma_{ext} + \sigma_{int}$ also has compressive character. Its value is even greater than the value of the thermal compressive stress. The lattice mismatch between sapphire and crystalline Si should cause compressive stress. Accordingly, the experimental results don't exclude the presence of such component in total stress. This may indicate that the origination of crystalline silicon phase takes place near the interface SiO_x:Er,F film/Al_2O_3 substrate.

5. Conclusions

Carried out investigations show considerable differences in the structure of non-doped and ErF_3-doped SiO_x films after thermal annealing. These differences consist in the greater facilitation of formation of Si nanocrystallites in the doped films, and may be attributed to the significant influence of fluorine on both the structure of as-prepared films and the nc-Si-crystallization process, as well as inhibiting action of fluorine against atmospheric oxygen. The results of this study also demonstrate the significant impact of the substrate on the nc-Si formation process in the course of SiO_x film decomposition into sub-phases. High compressive stress in nc-Si on sapphire substrate is determined by the fact that all three possible contributions to the total stress in these particles have compressive character. Analysis of our experimental results and literature data makes it possible to conclude that all three components are significant.

Acknowledgments

The authors are thankful to Prof. N. A. Vlasenko and Dr. Hab. V. Ya. Bratus' for helpful discussions.

References

[1] M. Sopinskyy, V. Khomchenko, Curr. Opin. Solid State Mater. Sci. **7**, 97 (2003).
[2] D. Pacifici, G. Franzo, F. Priollo, F. Iacona, L. Dal Negro, Phys. Rev. B **67**, 245301 (2003).
[3] D. Pacifici, A. Irrera, G. Franzo, M. Miritello, F. Iacona, F. Priolo, Physica E **16**, 331 (2003).
[4] Y. K. Fang, C. Y. Lin, S. F. Chen, C. S. Lin, T. H. Chou, International Electron Devices and Materials Symposia, IEDM 2006, Tainan, Proceedings, 443 (2006).
[5] F. Flores Gracia, M. Aceves, J. Carrillo, C. Domínguez, C. Falcony, Superfices y Vacio **18**(2), 7 (2005).
[6] R. Kiebach, J. A. Luna-López, G. O. Dias, M. Aceves-Mijares, J. W. Swart. J. Mex. Chem. Soc. **5**, 212 (2008).
[7] M.V. Sopinskyy, I. Z. Indutnyi, K. V. Michailovska, P. E. Shepeliavyi, V. M. Tkach**,** Semicond. Phys. Quant. Electron. Optoelectron. **14**, 273 (2011).
[8] R. A. Johnson, P. R. de la Houssaye, M. E. Wood, G. A. Garcia, C. E. Cheng, P. M. Asbeck, I. Lagnado, Electron. Lett. **33**, 1324 (1997).
[9] J. Roig, D. Flores, S. Hidalgo, J. Rebollo, J Millan, Microelectronics Journal **35**, 291 (2004).
[10] N. Karpov, V. Volodin, J. Jedrzejewski, E. Savir, I. Balberg, Y. Goldstein, T. Egewskaya, N. Shwartz, Z. Yanovitskaya, J. Optoelecrton. Adv. Mater. **11,** 625 (2009).
[11] M. Marinov, N. Zotov, Phys. Rev. B **55**, 2938 (1997).

[12] N. M. Liao, W. Li, Y. J. Kuang, Y. D. Jiang, S. B. Li, Z. M. Wu & K. C. Qi, Sci. China Ser. E – Tech. Sci. **52** , 339 **(**2009).
[13] W. Wei, G. Xu, J. Wang, T. Wang, Vacuum **81**, 656 (2007).
[14] N. Zotov, M. Marinov, N. Mousseau, G. Barkema, J. Phys: Condens. Matter. **11**, 9647 (1999).
[15] E. Bustarret, M. A. Hachicha, M. Brunel, Appl. Phys. Lett. **52**, 1675 (1988).
[16] H. Richter, Z. P. Wang, L. Ley, Solid State Commun. **39**, 625 (1981).
[17] I.H. Campbel, P.M. Fauchet, Solid State Commun. **58**, 739 (1986).
[18] G. Viera, S. Huet, L. Boufendi, J. Appl. Phys. **90**, 4175(2001).
[19] I. De Wolf, Semicond. Sci. Technol. **11**, 139 (1996).
[20] P.I. Didenko, A. A. Efremov, V. S. Khomchenko, G. Ph. Romanova, N. A. Vlasenko. Phys. Stat. Sol. A **100**, 501 (1987).
[21] N. A. Vlasenko, G. Ph. Romanova, B. V. Fenochka, V. S. Khomchenko, J. Luminesc. **40–41**, 792 (1988).
[22] R. E. Thoma, Rare-eath halides. Publisher: Oak Ridge, Tenn.: Oak Ridge National Laboratory, 1965.
[23] K. Vollenweider, B. Sahli, W. Fichtner, Phys. Rev. Lett. **103**, 075503 (2009)
[24] S. E. Kim, C. Steinbruchel, Appl. Phys. Lett. **75**, 1902 (1999).
[25] M. J. Shapiro, T. Matsuda, S. V. Nguyen, C. Parks, C. Dziobkowski, J. Electrochem. Soc., **143**, L156 (1996).
[26] Y. Ono, M. Tabe, Y. Sakakibara, Appl. Phys. Lett. **62**, 375 (1993).
[27] P. Ashburn, H. A. W. El Mubarek, J. Telecommun. Inform. Technol. **2/1997**, 3 (1997).
[28] V. Ya. Bratus, private communication.
[29] N. A. Vlasenko, N. V. Sopinskii, E. G. Gule, V. V. Strelchuk, P. F. Oleksenko, L. I. Veligura, A. S. Nikolenko, M. A. Mukhlyo, Semiconductors, **46,** 323 (2012).
[30] N. A. Vlasenko, L. I. Veligura, Z. L. Denisova, M. A. Mukhlyo, Yu. A. Tsyrkunov, V. F. Zinchenko, J. Soc. Inform. Display **14**, 615 (2006).
[31] [G. L. Olson, J. A. Roth. Mater. Sci. Rep. **3**, 1 (1988).
[32] J. S. Vainshtein, O. I. Kon'kov, A. V. Kukin, O. S. El'tsina, L. V. Belyakov, E. I. Terukov, O. M. Sreseli, Semiconductors **45**, 302 **(** 20011).
[33] P. G. Sennikov, S. V. Golubev, V. I. Shashkin, D. A. Pryakhin, M. N. Drozdov, B. A. Andreev, Yu. N. Drozdov, A. S. Kuznetsov, H. J. Pohl, JETP Lett. **89**, 73 (2009).
[34] G. Bruno, P. Capezzuto, M. M. Giangregorio, G. V. Bianco, M. Losurdo, Phil. Mag. **89**, 2469 (2009).
[35] M. S. Valipa, S. Sriraman, E. S. Aydil, D. Maroudas, J. Appl. Phys. **100**, 053515(2006).
[36] U. Kroll, J. Meier, A. Shah, S. Mikhailov, J. Weber, J. Appl. Phys. **80**, 4971 (1996).
[37] A.G. Hamers, A. Fontcuberta i Morral, C. Niikura, R. Brenot, P. Roca i Cabarrocas, J. Appl. Phys. **88**, 3674 (2000).
[38] H Fujiwara, M. Kondo, A. Matsuda, J. Non-Cryst. Solids **338-340**, 97 (2004).
[39] K. Christova, S. Alexandrova, A. Abramov, E. Valcheva, B. Ranguelov, C. Longeaud, S. Reynolds, P. Roca i Cabarrocas, J. Phys.: Conf. Ser. **253,** 012056 (2010).
[40] P. Lengsfeld, N. H. Nickel, Ch. Genzel, W. Fuhs, J. Appl. Phys. **91**, 9128 (2002).
[41] S. Wolf, R. N. Taubner, in: Silicon Processing for the VLSI Era. Vol. I: Process Technology (Lattice, Sunset Beach, CA, 1986).
[42] S. Cristovianu, Rep. Prog. Phys. **50**, 327 (1987).
[43] S. Yerci, U. Serincan, I. Dogan, S. Tokay, M. Genisel, A. Aydinli, R. Turan, J. Appl. Phys. **100**, 074301 (2006).
[44] S. Sahoo, S. Dhara, S. Mahadevan, A. K. Arora, J. Nanosci. Nanotechn. **9**, 5604 (2009).

*Corresponding author: sopinsky@isp.kiev.ua, sopinskyy@ua.fm